JOURNAL OF AGRICULTURAL AND FOOD CHEMISTRY
ARTICLE

J. Agric. Food Chem. 2009, 57, 6997–7004 6997
DOI:10.1021/jf901432h

Gel-Based Proteomics Approach to the Study of Metabolic Changes in Pear Tissue during Storage

Romina Pedreschi,*[,†] Maarten Hertog,[†] Johan Robben,[‡] Kathryn S. Lilley,[§] Natasha A. Karp,[§,#] Geert Baggerman,[∥] Jozef Vanderleyden,[⊥] and Bart Nicolaï[†]

[†]BIOSYST-MeBioS Division, Katholieke Universiteit Leuven, Leuven, Belgium, [‡]Biochemistry, Molecular, and Structural Biology Section, Katholieke Universiteit Leuven, Leuven Belgium, [§]Department of Biochemistry, University of Cambridge, Cambridge, U.K., [∥]Prometa, Katholieke Universiteit Leuven, Leuven, Belgium, and [⊥]Centre of Microbial and Plant Genetics, Katholieke Universiteit Leuven, Leuven, Belgium. [#]Present address: Mouse Genetic Program, Welcome Trust Sanger Institute, U.K

The effect of extreme gas conditions (anoxia and air) on the protein expression profiles of Conference pear slices was assessed with a differential gel electrophoresis (DIGE) approach using robust statistical analysis. Changes in expression, up to 4-fold, were identified in proteins involved in respiration, protein synthesis, and defense mechanisms. In addition, short-term exposure of pear slices to anoxia clearly induced up-regulation of transketolase and polygalacturonase inhibiting protein and down-regulation of several isoforms of the major allergen Pyrc (PR proteins), providing further evidence of the possible involvement of these enzymes in the development of the physiological disorder core breakdown. The role of these PR proteins under anoxia is unknown, but our results suggest that these proteins are involved in protection against abiotic stress such as the anoxic conditions applied.

KEYWORDS: Controlled atmosphere; LC-ESI-MS/MS; *Pyrus communis* L; multivariate statistics; proteomics; spot overlap; PR proteins

INTRODUCTION

Horticultural crops are constantly exposed to abiotic stresses. During harvesting and handling, a series of mechanical stresses are imposed on the plant cells that induce different cellular responses such as increased respiration rate, ethylene production, higher susceptibility to pathogen attack, and wound responses. These all lead to a reduction of the quality and storability of the crops (*1*, *2*). Further, horticultural crops are highly perishable after harvest and require special techniques to avoid rapid deterioration. Controlled atmosphere (CA) storage is commonly applied to horticultural crops such as apple and pear to extend their shelf lives. It involves temperature reduction and modification of the air composition (oxygen reduction and carbon dioxide increase) in order to retard respiration, ethylene production, and senescence (*3*). However, these CA conditions may impose additional abiotic stresses when the oxygen and carbon dioxide partial pressures are too low or too high, respectively. Different physiological disorders associated with improper CA management have been reported such as chilling injury, failure to ripen, development of off flavors, (*4*, *5*) and browning disorders (*6*). These disorders are generally poorly understood from a physiological point of view. To improve our understanding, there is need for more holistic approaches such as the use of high throughput techniques like proteomics or metabolomics (*7*−*10*).

Pome fruits, apple, and pear are native to most of Europe, the Near East, and Asia. In terms of world production, they are considered among the major four fruit classes and the second major fruit in moderate climates (*11*). Specifically, the pear variety "Conference" is highly susceptible to internal browning and to subsequently develop core breakdown during CA storage (*6*). Core breakdown has been shown to be related to the gas composition in the storage atmosphere (*12*); thus, much attention has been paid to the mechanisms of gas transport in the fruit (*13*−*16*) and the microstructure of the intercellular space as the main transport path for metabolic gases (*17*). A previous proteomics study on core breakdown in "Conference" pears characterized the most relevant proteins involved in this disorder (*7*). Internal browning and core breakdown in Conference pears are believed to be the result of an imbalance between oxidative and reductive processes due to the formation of gas gradients in the fruit inducing accumulation of reactive oxygen species leading to membrane damage finally resulting in the enzymatic oxidation of polyphenols to brown colored compounds (*6*). Although it is generally accepted that suboptimal or extreme CA conditions trigger core breakdown (*6*), proteomics studies focusing on extreme gas concentrations which are believed to play a major role in the appearance of the disorder have not been carried out yet.

In an attempt to understand the effect of the CA composition on the metabolism of "Conference" pear, regardless of time and actual browning development, the current study focuses on

*To whom correspondence should be addressed. Address: Food Safety and Quality Unit, Institute for Reference Materials and Measurements, Joint Research Centre, European Union, Retieseweg 111, B-2440, Geel, Belgium. E-mail: romina.pedreschi@ec.europa.eu. Phone: + 32 14 57 1829. Fax: +32 14 57 1787.

Published on Web 07/02/2009

protein expression changes in thin pear slices submitted to extreme gas compositions using two-dimensional differential gel electrophoresis (2-DE DIGE) combined with a rigorous statistical analysis of the data preceding LC−ESI-MS/MS identification of the relevant proteins. With the introduction of more sensitive MS equipment, spot overlap becomes evident in 2-DE protein separation (*18*, *19*). Within a spot with several protein identifications, the one involved in the regulation could be incorrectly assigned. More frequently the information is discarded, as it is unclear which protein species has the highlighted fold change or even whether the fold change is a composite for different proteins each with differing relative expression levels. Different approaches to counteract the problem involve the use of narrow range immobilized pH gradient (IPG) strips, sample fractionation methods, different sample preparation conditions, and modification of conditions during 2-DE (*19*). We propose that the use of spectral counts can help to identify which protein species within a spot is the most abundant protein accounting for the changes observed. Spectral counting consists of counting the total number of spectra representing identified peptides for a certain protein (*20*, *21*) and has been shown to correlate closely with protein concentration (*20*).

The results from this study not only picture the short-term effect of gas composition on the metabolism of CA stored pears but also highlight the need to carry out an extensive and complete analysis of the data to draw sound conclusions. Knowledge of how horticultural crops respond to environmental changes and industrial manipulation is of key importance for quality assurance and process optimization in the food industry (*1*). The same approach could potentially be applied to other commodities in order to come up with solutions to the different problems faced by the postharvest industry to reduce economic losses.

MATERIALS AND METHODS

Plant Material. Pears (*Pyrus communis* cv. Conference) were harvested in the orchard of the Centre for Fruit Culture in Rillaar (Belgium). All pears were stored under optimal controlled atmosphere (CA) conditions. Pears were picked at the commercial harvest date on September 16, 2006, as determined by the Flanders Centre of Postharvest Technology (Belgium). The fruit was submitted to precooling in air at −1 °C for 3 weeks before applying optimal controlled atmosphere conditions of 2.5% O_2 and 0.7% CO_2 at −1 °C following commercial protocols. Pears were stored for 8 months under these commercial storage conditions, as pears stored for longer periods are more likely to develop core breakdown disorder.

Sample Preparation. Pears taken from the commercial storage conditions were cut perpendicularly to the stem−calyx axis at 5 cm from the calyx. Samples were taken rapidly in a cooling room at 1 °C to prevent oxidation. Thin slices of tissue samples (1.5 mm thick and 2.5 cm diameter) were taken from the equatorial region excluding the skin and core. For each condition, 1.5 L respiration jars were filled with 150 g of pear tissue slices distributed over six metal grids each carying one layer of tissue slices equally spaced and without overlap. The 1.5 L jars were connected in series. CA conditions of 20% O_2 and 80% N_2 (air) and 10% CO_2 and 90% N_2 (anoxia) were generated to flush the jars at 10 L/h. Before entering the jars, the CA mixtures were humidified. Gas composition was monitored using a PBI Dansensor, model Chekmate no. O2 (Zr) CO_2-100% (Denmark). The control consisted of pear slices from pears coming directly from the commercial storage, and they were immediately frozen in liquid nitrogen until further analysis. Jars were incubated at 1 °C for 5 days. In all cases four independent biological replicates composed of slices from 10 sampled pears were obtained for each condition (control, air, and anoxia).

Protein Extraction and CyDye Labeling. Proteins were extracted using a phenol extraction followed by precipitation in 100 mM ammonium acetate in methanol as detailed in ref 7. The obtained protein pellets were stored at −80 °C until analysis. Total protein concentrations were determined using the Bio-Rad DC protein assay following the manufacturer's guidelines (Bio-Rad, UK).

The protein pellets were rehydrated in DIGE buffer (7 M urea, 2 M thiourea, 4% CHAPS, 5 mM magnesium acetate, 10 mM Tris, pH 8.0). The pH was adjusted to 8.5 using a 50 mM NaOH solution. Proteins were labeled using the fluorescent cyanine dyes developed for DIGE (GE Healthcare) following the manufacturer's guidelines. Thus, an amount of 50 μg of proteins was labeled with 400 pmol of amine reactive cyanine dyes dissolved in fresh anhydrous dimethylformamide. The two-dye approach recommended by Karp et al. (*22*) was used. Four biological replicates per treatment (control, air, or anoxia) were independently labeled with Cye 3. Cye 5 was used to label the internal standard composed of equal amounts of all samples. The labeling reaction was incubated in the dark for 30 min and quenched with 10 nmol of lysine. An equal volume of 2× sample buffer (7 M urea, 2 M thiourea, 4% CHAPS, 20 mg/mL DTT, and 2% Pharmalites 3-10) was added to each of the labeled samples. Rehydration buffer (7 M urea, 2 M thiourea, 4% CHAPS, 10 mg/mL, and 1% Pharmalites 3-10) was added to make up a final volume of 450 μL prior to IEF. The Pharmalites 3-10 was obtained from Bio-Rad. Both the internal standard labeled with Cye 5 and the sample labeled with Cye 3 were mixed and run together in the same gel.

Two-Dimensional Gel Electrophoresis. Linear IPG strips (24 cm long) of pH 4−7 (GE Healthcare) were rehydrated with the CyeDye labeled samples for 10 h at 20 °C at 20 V using the IPGphor II apparatus (GE Healthcare). The steps of the IEF included 1 h at 500 V, 1 h at 1000 V followed by 8.2 h at 8000 V. The last step consisted of 24 000 V h at 8000 V. After IEF completion, strips were equilibrated individually for 15 min in 10 mL of equilibration buffer (8 M urea, 30% glycerol, 1% SDS, 100 mM Tris-HCl, pH 6.8) containing 2% w/v DTT and subsequently for 15 min in 10 mL of equilibration buffer containing 2.5% iodoacetamide. Second dimension separation was performed in an Ettan DALT Twelve system (GE Healthcare) with lab cast 1.0 mm SDS polyacrylamide gels (12.5%). Gels were run overnight at 1.5 W/gel.

Protein Visualization and Image Analysis. Labeled proteins were visualized in a Typhoon 9410 imager (GE Healthcare). Cye 3 images were scanned using a 532 nm laser and 580 nm band-pass (BP) emission filter. Cye 5 images were scanned using a 633 nm laser and a 670 nm BP30 emission filter. Gels were scanned at a 100 μm resolution. The photomultiplier tube (PMT) was set to ensure maximum pixel intensity between 40 000 and 60 000 pixels. Gel analysis was performed using Progenesis SameSpots (Nonlinear Dynamics, U.K.), a 2-DE analysis software package.

Data Analysis. A complete statistical analysis was carried out using both univariate and multivariate statistics on the log standardized abundance where the log standardized abundance is the Cye 3 sample spot volume divided by the Cye 5 standard sample spot volume after ratiometric normalization. By use of both approaches independently, not only absolute changes in terms of protein expression but also correlations and concerted changes in expression can be assessed.

Univariate Statistics. One-way analysis of variance (ANOVA) was carried out at $p < 0.01$ and $p < 0.05$ in order to assess for absolute protein changes among the different treatments. The false discovery rate (FDR) was assessed by calculating q-values using the p-values (*23*); consequently, both a p-value and a q-value are calculated for each spot. The q-value is a measure of significance in terms of FDR. Since the q-value approach relies on the use of the correct statistical test (one-way ANOVA) for the experimental design (*22*), the two-dye DIGE schema was used as outlined in the protein extraction and CyDye labeling section. By calculating the q-values, the user has control over the FDR because differing p-value thresholds can be chosen for differing levels of false call rates. The FDR estimates how many, from the spots declared to be significant by the one-way ANOVA test, are expected to be not significant at all. Differentially expressed proteins were manually checked as being proper spots before submitting them for protein identification. Pairwise comparisons were carried out by using a Tukey test ($p < 0.05$) in SPSS, version 15 (Chicago, IL) only on those proteins declared to be significant by one-way ANOVA.

Multivariate Statistics. Data preprocessing steps included mean centering and standardizing the variance. Principal component analysis (PCA), an unsupervised technique, was carried out as a first exploration of the data and to identify possible outlying gels through the 95% Hotelling's

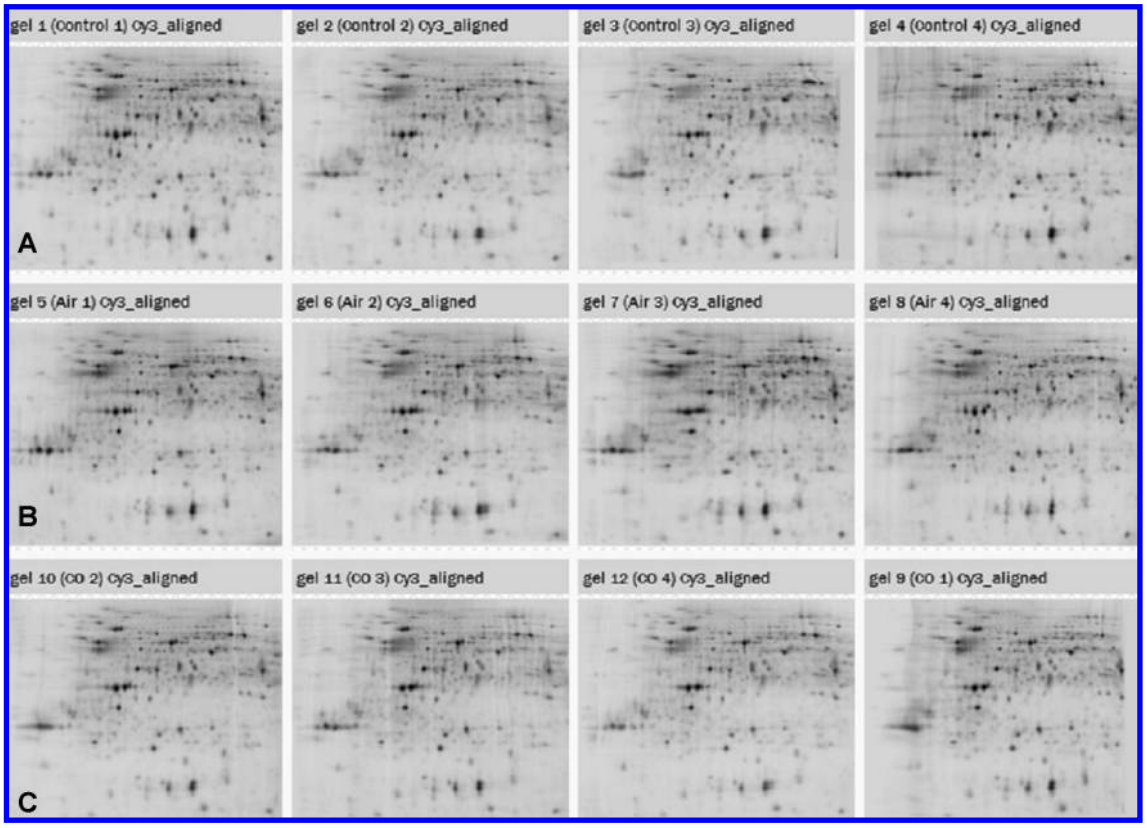

Figure 1. 2-DE DIGE maps for the different applied treatments: (**A**) control (2.5% O_2, 0.7% CO_2); (**B**) high oxygen or air (20% O_2); (**C**) high carbon dioxide or anoxia (10% CO_2). Four independent biological replicate gels are displayed per treatment.

T^2 limit (*24*). Partial least-squares discriminant analysis (PLS-DA) analysis, a supervised technique, was carried out to sharpen the discrimination among the treatments according to similar protein expression profiles as detailed in ref *8*. The variable importance plot (VIP) was used as formal tool based on the correlation loadings to identify the most relevant proteins involved in class distinction. Further details can be found in refs *7* and *8*. The VIP procedure was first run to select the 120 most important proteins. Selected proteins were manually checked as being real spots. Real spots were confirmed, and the VIP procedure was run again with these proteins. Only proteins successfully identified by LC−ESI-MS/MS that were independently selected from the univariate ($p < 0.05$ and $q < 0.1$) and multivariate statistical analysis were used to build the final PLS-DA model. Because of the small number of observations, cross-validation was applied to test the performance of the models. PCA and PLS-DA analyses were performed using Unscrambler 9.6 (CAMO A/S, Trondheim, Norway).

Protein Identification. Mass spectrometry experiments were performed using an LTQ linear ion trap instrument fitted with a nanospray ion source (ThermoFisher, Waltham, MA) as detailed in ref *25*. Since the number of *Pyrus communis* sequences in the public databases is very limited, MS/MS data analysis and cross species ID were applied for protein identification. Data were submitted to the Mascot search algorithm (Matrix Science, London, U.K.) and searched against the GenBank nonredundant Viridiplantae-specific protein sequence database, using a fixed modification of carbamidomethyl and a variable modification of oxidation (M). In a second identification round, a Mascot search was performed against the *Malus* × *domestica* EST sequences from Unigene database of December 8, 2007. Proteins assigned on the basis of two or more peptides were considered as confidently identified. When more than one protein was assigned within a spot, spectral counting was used as a rough estimate of protein abundance (*20*).

RESULTS

Even though extreme gas conditions were applied, the effect of the different treatments did not trigger large visual changes in protein expression (**Figure 1**). Quantitatively it was found that the observed fold changes in protein expression levels were limited to a maximum of 4.

Selected Spots through Univariate Statistics. The one-way ANOVA revealed 105 significant spots at a $p < 0.01$ value from which 56 were confirmed as real spots and suitable for identification. By application of the false discovery rate approach with a q-value threshold of 0.05, 6 out of the 56 were estimated to be false positives.

Selected Spots through Multivariate Statistics. The PCA model generated with all variables included revealed already a good discrimination among the different treatments (PC1 and PC2 were able to explain 22% and 14% of the total variance) (Supporting Information). No outlying gels were found. A PLS-DA model as a supervised technique sharpened the discrimination among the treatments, and further analysis focuses on this multivariate technique. The PLS-DA model with all spot data revealed good discrimination among the different gas conditions, being able to explain 93% of the observed variation between the treatments based on the first two latent variables (Supporting Information). In order to narrow the number of proteins selected for further work, a new PLS-DA model was built based only on the 120 most important spots selected through the VIP procedure. This reduced model was still able to explain 86% of the variation between the treatments with the first two latent variables (Supporting Information).

Bringing Both Statistical Approaches Together. From the 105 spots selected through one-way ANOVA ($p < 0.01$), 75 were also selected through PLS-DA and VIP 120 procedure. Of the 120 spots chosen by the VIP procedure 112 spots had a $p < 0.05$ value. Univariate and multivariate approaches are different, thus, the explanation for the slightly different selection of spots for both

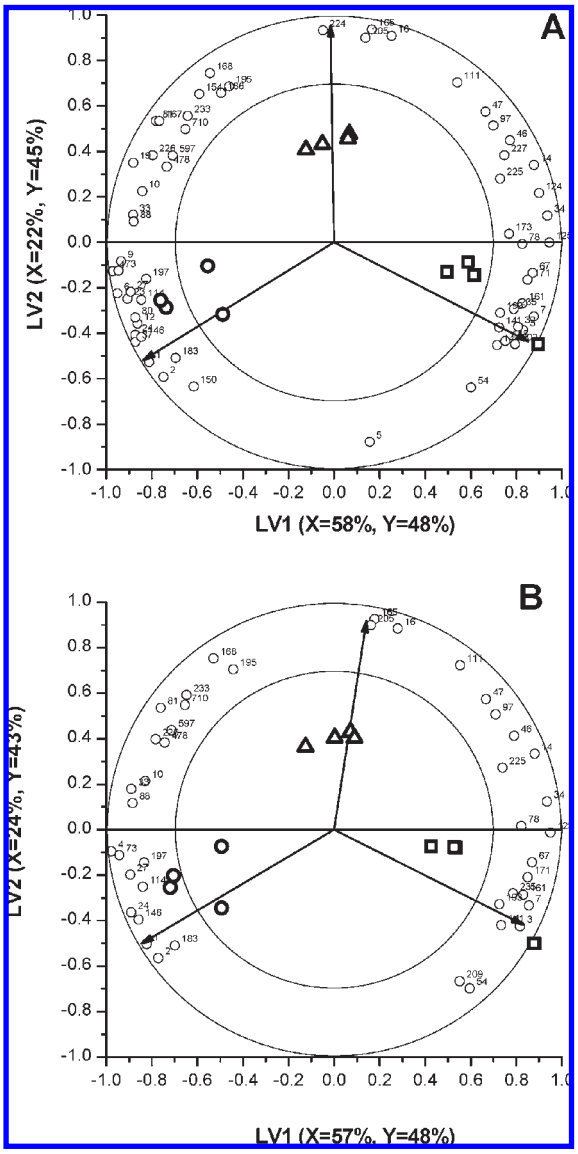

Figure 2. PLS-DA biplot built with the (**A**) 63 proteins selected through univariate and multivariate statistics and sent for LC−ESI-MS/MS identification and (**B**) 43 identified proteins considered as singlets. Sample scores and loadings (proteins) are superimposed. The percentage explained variances are indicated on the axes. The analysis was based on the correlation matrix. Open small circles represent the different proteins. Squares represent control (2.5% O_2, 0.7% CO_2) conditions, circles represent high oxygen or air (20% O_2) conditions, and triangles represent high carbon dioxide or anoxic (10% CO_2) conditions.

approaches. PLS-DA accounts for correlations while ANOVA not. Thus, highly correlated proteins even though not with high fold changes will get a high loading and thus not found to be differentially expressed by ANOVA. Spots that were identified as significant by either the univariate or the multivariate method were sent for MS identification after confirming they were real spots. Only 63 spots have been analyzed because of technical problems. Thus, 63 spots were submitted for identification, out of which 43 spots were selected by both approaches and a new PLS-DA model based on these proteins was built (**Figure 2A**). The remaining spots were excluded from the analysis. Focusing the multivariate technique on the spots that provide the discrimination allows a clear visualization as to which proteins species contribute to the separation in the multivariate space. The explained variance between the treatments was 93%, accounting for the two first latent variables when the 63 spots were included. The remaining variation was still very well explained by the remaining real 43 proteins obtaining a good discrimination between the treatments (**Figure 2B**).

LC−ESI-MS/MS Identification of Selected Spots and Correlation Patterns. The statistically relevant spots selected through univariate and multivariate tools were analyzed by LC−ESI-MS/MS. Fifty-three out of 63 spots (84%) yielded a confident match with pear or protein sequences from GenBank. The additional Mascot search against the apple EST database confirmed most of these identifications and increased the identification rate to 94% (59 out of 63 proteins). The use of Malus ESTs is a valuable source data for the investigation of the poorly documented pear proteome. The complete list of investigated spots and confidently identified peptides together with their statistical scores is provided in Supporting Information (**Table 1**). The presence of multiple proteins within a spot was clearly evident from the identifications (**Figure 3**). Thus, spectral counts were used as a rough estimate of protein abundance. Within a spot with multiple protein identifications, if the total number of spectral counts was significantly higher for a certain identification (> 70%), it was considered as a singlet (Supporting Information table). The PLS-DA model built with singlets is shown in **Figure 2B**.

Identified proteins belong to different categories with different biological functions such as central metabolism, defense mechanisms, and protein synthesis. Their roles and the interconnection among pathways are further elaborated in the Discussion.

DISCUSSION

Statistical Analysis. The high level of overlap of species identified as significant between the univariate and multivariate technique demonstrates the robustness of the technique and gives confidence that highly significant changes are being identified. There was a 60% overlap between the proteins selected through one-way ANOVA ($p < 0.01$) and PLS-VIP 120 and 95% at a p-value of 0.05 for the one-way ANOVA selection. The unsupervised PCA technique revealed a good discrimination among the different treatments, validating that the model was correct. Use of the supervised PLS-DA technique sharpened the discrimination among the treatments. The biplots (**Figure 2A** and **Figure 2B**) show the marked discrimination among the treatments, as evidenced by the tight clusters formed among the three treatments and their separation along LV1 and LV2, respectively. The latent variable 1 (LV1) of the PLS-DA model is able to explain the variation between the control and oxygen, while the latent variable 2 (LV2) explains the variation between the control and anoxia. On the basis of the marked discrimination of the treatments, it can be clearly observed that certain proteins are clearly characteristic or highly correlated to a specific treatment.

Spot Overlap Deserves Special Attention. With the introduction of more sensitive MS equipment, spot overlap has become more evident in 2-DE protein separation (*26*, *27*). This issue represents a serious problem in terms of relative quantification for further biological interpretation of the data. The presence of several proteins within a spot arises, as in practice more than one protein can migrate to the same location on a 2-DE gel because of the large dynamic range of proteins within a cell. Additionally, unresolved proteins might be accompanied by contaminants. Different approaches to counteract the problem involve the use of narrow range IPG strips, sample fractionation methods, different sample preparation conditions, and modification of conditions during 2-DE (*19*). As pear proteome is poorly characterized, the use of gel-free approaches is not a feasible alternative,

Table 1. Summary of the Proteins Considered as Singlets and Chosen through One-Way ANOVA, PLS-DA, and VIP Procedure[a]

protein name	spot ID	protein ID	*p*-value	*q*-value	power	log of standarized abundance (SA) ± standard error (SE) control	air	high CO_2
1. Metabolism								
ATP synthase subunit d, mitochondrial	225	Mdo. 7184	0.019	0.07	0.77	$0.030^{a} \pm 0.008$	$-0.017^{b} \pm 0.013$	$0.018^{a,b} \pm 0.007$
pyruvate dehydrogenase E1 β subunit	161	Mdo. 3217	0.011	0.06	0.85	$0.027^{a} \pm 0.022$	$-0.048^{b} \pm 0.006$	$-0.030^{b} \pm 0.008$
ADP glucose synthase (*)	88	Mdo. 1894	0.005	0.038	0.93	$-0.065^{a} \pm 0.021$	$0.048^{b} \pm 0.021$	$-0.000^{a,b} \pm 0.009$
acetyl CoA acetyl transferase (*)	27	Mdo. 9294	0.001	0.018	0.99	$-0.089^{a} \pm 0.033$	$0.118^{b} \pm 0.027$	$-0.032^{a} \pm 0.0222$
phosphoglycerate dehydrogenase like	81	Mdo. 10865	0.000	0.002	1.00	$-0.093^{a} \pm 0.010$	$0.012^{b} \pm 0.009$	$0.0267^{b} \pm 0.013$
aconitase	226	Mdo. 12067	0.004	0.033	0.95	$-0.022^{a} \pm 0.006$	$0.021^{b} \pm 0.008$	$0.015^{b} \pm 0.006$
transketolase (*)	125	3559814	0.000	0.006	1.00	$0.074^{a} \pm 0.011$	$-0.020^{b} \pm 0.005$	$0.024^{c} \pm 0.011$
NADP-dependent malic enzyme (*)	233	Mdo. 12341	0.040	0.104	0.63	$-0.048^{a} \pm 0.009$	$-0.020^{a,b} \pm 0.005$	$-0.014^{b} \pm 0.009$
NADP-dependent malic enzyme	710	Mdo. 11996	0.092	0.149	0.46	$-0.066^{a} \pm 0.025$	$-0.018^{a} \pm 0.008$	$-0.016^{a} \pm 0.006$
enolase (*)	24	Mdo. 11920	0.000	0.004	1.00	$-0.072^{a} \pm 0.029$	$0.161^{b} \pm 0.016$	$-0.059^{a} \pm 0.023$
phosphoglycerate kinase	168	Mdo. 2160	0.003	0.030	0.96	$-0.053^{a} \pm 0.015$	$-0.011^{b} \pm 0.009$	$0.019^{b} \pm 0.005$
phosphoglycerate kinase	195	Mdo. 2160	0.009	0.052	0.88	$-0.048^{a} \pm 0.011$	$-0.014^{a,b} \pm 0.007$	$0.013^{b} \pm 0.013$
malate dehydrogenase (*)	46	Mdo. 15920	0.001	0.018	0.99	$0.048^{a} \pm 0.016$	$-0.1270^{b} \pm 0.036$	$0.039^{a} \pm 0.018$
enolase (*)	33	Mdo. 11920	0.011	0.058	0.85	$-0.131^{a} \pm 0.042$	$0.065^{b} \pm 0.025$	$-0.022^{a} \pm 0.035$
2. Protein Folding and Stabilization								
heat shock protein HSP 70	54	Mdo. 1243	0.043	0.104	0.62	$0.066^{a} \pm 0.051$	$-0.037^{a,b} \pm 0.030$	$-0.082^{b} \pm 0.015$
heat shock protein HSP 70	478	Mdo. 1243	0.082	0.134	0.49	$-0.066^{a} \pm 0.036$	$0.018^{a} \pm 0.018$	$-0.003^{a} \pm 0.009$
heat shock protein HSP 90	171	Mdo. 423	0.011	0.059	0.84	$0.059^{a} \pm 0.013$	$-0.011^{b} \pm 0.011$	$0.011^{a,b} \pm 0.014$
ATP binding/GRP 94 homologue	209	Mdo. 423	0.041	0.104	0.63	$0.048^{a} \pm 0.016$	$0.014^{a,b} \pm 0.013$	$-0.006^{b} \pm 0.006$
3. Protein Synthesis								
translation initiation factor eIF-5A-2 (*)	16	77555893	0.000	0.000	1.00	$-0.035^{a} \pm 0.012$	$-0.118^{b} \pm 0.016$	$0.166^{c} \pm 0.018$
nuclei acid binding protein	78	Mdo. 6093	0.005	0.037	0.93	$0.101^{a} \pm 0.019$	$-0.024^{b} \pm 0.027$	$0.024^{a,b} \pm 0.008$
translation elongation factor G	193	Mdo. 6297	0.008	0.048	0.89	$0.054^{a} \pm 0.015$	$-0.009^{b} \pm 0.012$	$-0.007^{b} \pm 0.009$
CDC 48 like protein	597	Mdo. 253	0.105	0.149	0.43	$-0.025^{a} \pm 0.030$	$0.039^{a} \pm 0.017$	$0.028^{a} \pm 0.005$
translation initiation factor eIF-4A (*)	14	Mdo. 5235	0.000	0.008	0.99	$0.112^{a} \pm 0.020$	$-0.190^{b} \pm 0.052$	$0.036^{a} \pm 0.006$
Translation initiation factor eIF-4A (*)	146	Mdo. 5235	0.000	0.002	1.00	$-0.050^{a} \pm 0.004$	$0.033^{b} \pm 0.007$	$-0.045^{a} \pm 0.010$
translation initiation factor eIF-4A (*)	73	Mdo. 5235	0.000	0.002	1.00	$-0.078^{a} \pm 0.013$	$0.049^{b} \pm 0.012$	$-0.031^{c} \pm 0.003$
4. Transport								
vacuolar ATPase subunit A	235	60592630	0.003	0.030	0.96	$0.020^{a} \pm 0.005$	$-0.010^{b} \pm 0.005$	$-0.006^{b} \pm 0.004$
5. Cellular Communication								
14−3−3 like protein (*)	205	Mdo. 5581	0.003	0.033	0.95	$-0.032^{a} \pm 0.007$	$-0.046^{a} \pm 0.013$	$0.010^{b} \pm 0.005$
6. Stress Related Proteins								
major allergen Mal d (*)	1	Mdo. 13717	0.000	0.001	1.00	$-0.198^{a} \pm 0.053$	$0.330^{b} \pm 0.016$	$-0.202^{a} \pm 0.050$
major allergen Mal d 1.03 (*)	4	Mdo. 13717	0.000	0.002	1.00	$-0.204^{a} \pm 0.035$	$0.224^{b} \pm 0.023$	$-0.040^{c} \pm 0.047$
major allergen Pyrc 1 (*)	183	3044216	0.007	0.047	0.90	$-0.001^{a} \pm 0.009$	$0.064^{b} \pm 0.013$	$-0.002^{a} \pm 0.015$
ACC oxidase (*)	47	4586409	0.000	0.013	0.99	$0.030^{a} \pm 0.021$	$-0.126^{b} \pm 0.024$	$0.044^{a} \pm 0.020$
polygalacturonase inhibiting protein (*)	165	33087506	0.000	0.013	0.99	$-0.026^{a} \pm 0.014$	$-0.044^{a} \pm 0.006$	$0.030^{b} \pm 0.001$
isoflavone reductase related protein	7	3243234	0.000	0.004	1.00	$0.316^{a} \pm 0.034$	$-0.039^{b} \pm 0.039$	$0.021^{b} \pm 0.033$
superoxide dismutase	141	Mdo. 1321	0.024	0.080	0.73	$0.105^{a} \pm 0.027$	$0.022^{b} \pm 0.008$	$0.030^{a,b} \pm 0.018$
7. Other Proteins								
endomembrane associated protein	3	Mdo. 7202	0.008	0.050	0.88	$0.216^{a} \pm 0.089$	$-0.233^{b} \pm 0.104$	$-0.174^{b} \pm 0.047$
hydrolase, hydrolyzying *O*-glycosyl (*)	34	Mdo. 16650	0.000	0.002	1.00	$0.102^{a} \pm 0.008$	$-0.091^{b} \pm 0.030$	$0.019^{c} \pm 0.008$
hydrolase, hydrolyzing *O*-glycosyl (*)	111	Mdo. 16650	0.002	0.026	0.97	$0.004^{a} \pm 0.017$	$-0.007^{b} \pm 0.016$	$0.033^{a} \pm 0.009$
hydrolase, hydrolyzing *O*-glycosyl	10	Mdo. 11995	0.000	0.006	1.00	$-0.143^{a} \pm 0.022$	$0.175^{b} \pm 0.040$	$0.118^{b} \pm 0.034$
progesterone 5-β reductase (*)	197	Mdo. 6425	0.005	0.038	0.93	$-0.019^{a} \pm 0.009$	$0.042^{b} \pm 0.012$	$0.002^{a} \pm 0.007$
Clp C protease	67	Mdo. 1094	0.001	0.017	0.99	$0.098^{a} \pm 0.007$	$-0.038^{b} \pm 0.022$	$-0.000^{b} \pm 0.019$
p-hydroxyphenyl pyruvate dioxygenase (*)	114	Mdo. 3417	0.003	0.028	0.97	$-0.040^{a} \pm 0.013$	$0.058^{b} \pm 0.021$	$-0.016^{a} \pm 0.002$
rubisco large subunit (*)	97	4098550	0.004	0.033	0.95	$0.003^{a} \pm 0.009$	$-0.102^{b} \pm 0.021$	$0.004^{a} \pm 0.022$

[a] The complete table can be accessed in Supporting Information. From the 63 proteins selected from independent univariate and multivariate statistical analysis, those proteins that were significantly different from the control and between the treatments by a pairwise comparison Tukey test ($p < 0.05$) are displayed with an asterisk. Different superscript letters account for statistical differences ($p < 0.05$).

since cross-species identification is the sole option for a poorly characterized genome. However, even when spot overlap exists, meaningful data can still be extracted. In this study, we used spectral counts to assign major proteins to spots with mixed spectra. Spectral counting involves counting the total number of spectra representing identified peptides for a certain protein (*20*, *21*). Almost 80% of the analyzed 63 proteins contained multiple proteins. By application of spectral counts as a rough estimate of protein abundance, 43 of the 59 successfully identified proteins were identified as singlets (**Figure 3** and Supporting

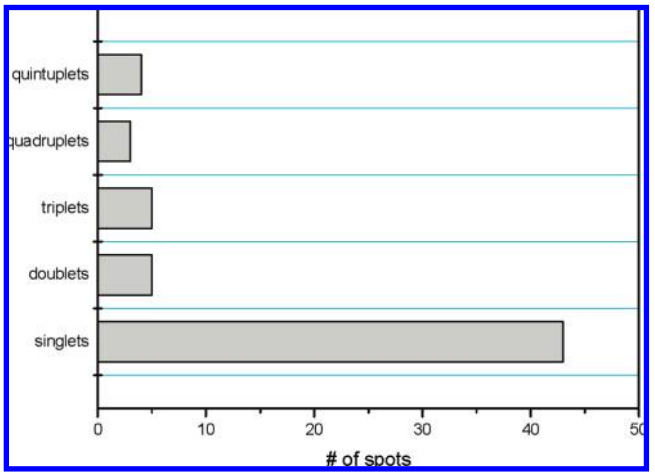

Figure 3. Representation of the number of singlets, doublets, triplets, quadruplets, and quintuplets found after LC−ESI-MS/MS identification and applying spectral counts as a rough indication of protein abundance.

Information table). To be considered as singlet, the top hit ranked protein represented at least 70% of the total spectral counts.

Spectral counts correlate well with protein concentration, in contrast to peptide counts that correlate poorly (*20*). However, there are certain shortcomings that must be mentioned such as the fact that the approximation of abundance from the repeat peptide observations per protein totally ignores the size of the protein; large proteins contribute with more peptides than small ones, resulting in an overestimation if the data are not normalized (*26*, *27*). The data should also be normalized for the expected number of tryptic peptides (*28*). Additionally, depending on the instrumental setup for data acquisition, some peptides will be detected more easily than others and others will never be detected even if they are abundant in the sample (*21*, *29*). The most typical setup consists of prior separation of the peptides in an ion exchange and/or reverse phase chromatography. By reduction of the complexity of the peptide mixture, the instrument is not overwhelmed by the most abundant species, making it possible to measure the less abundant ones. In a data-dependent mode, there are peptides that are difficult to detect either because they are difficult to ionize or fragment or because they coelute with abundant peptides. Thus, these peptides are rarely selected by the instrument. These peptides are poor abundance reporters because the number of times they are detected remains almost constant or only changes for strong concentration changes (*29*).

Recently, Yang et al. (*30*) has successfully applied an exponentially modified protein abundance index (emPAI) to determine the abundance of the individual proteins comprised within a spot containing multiple proteins. Although spectral counts correlate very well to protein abundance, they might not necessarily correlate very well to spot volume (e.g., minor protein components in terms of abundance might be more effectively labeled and thus account for most of the fluorescent signal).

Biological Interpretation. From the 43 identified singlets by spectral counts, a subselection of proteins for biological interpretation (**Table 1**) has been based on Tukey pairwise comparisons ($p < 0.05$) following two main criteria: at least one of the treatments should differ from the control, and there should be statistical differences between the treatments. The selected proteins have been classified on the basis of their function and discussed accordingly. All comparisons are referenced to control conditions.

Central Metabolism. Only subtle changes were observed at the glycolytic and Krebs cycle pathways. The main changes observed correspond to the slight up-regulation of malic enzyme (spot 233). This can be seen as a way to circumvent the dependence on glycolysis to generate ATP by instead using the reserves of malic acid already present in the tissue. Similar results were obtained with whole pears exposed to browning inducing conditions (*7*). This reaction of the malic enzyme is also important in producing reducing equivalents such as NADPH, needed by defense related pathways such as the glutathione−ascorbate pathway.

In addition, an up-regulation of transketolase was observed (spot 125). This finding provides further evidence to a previous metabolomics study in which there was pentose phosphate pathway activation under anoxic conditions (*10*). The oxidative part of the pentose phosphate pathway is a major source of NADPH which is used for the synthesis of fatty acids and is important for the maintenance of the redox potential to protect against oxidative stress (*31*).

Previous work with whole pears stored under browning inducing conditions (*7*, *9*) revealed that respiration pathways were at least partially involved in the appearance of core breakdown disorder in Conference pears. These results provide extra evidence of the direct response of respiration involved enzymes to short-term exposures to changed gas conditions before core breakdown is evident.

In summary, central metabolism pathways seem to be altered in the short term exposure of pear slices to the tested gas conditions. Although this discussion focuses on a limited number of selected proteins, these proteins are the ones from the full proteome that were shown to be significantly affected. Of course, subtle changes that did not get beyond the noise level might be missing.

Defense Related Proteins. Non-significant changes were observed in the ascorbate−glutathione cycle, while changes in the regulation of several PR proteins (known as allergens) and PGIP were significant. Thus, we suspect that browning really starts as soon as the ascorbate−glutathione cycle collapses (*7*). The most pronounced changes in expression of proteins due to air or anoxic conditions were found with a series of PR isoforms. They were consistently up-regulated in air conditions during the 5-day exposure of pear slices (**Table 1**) and highly correlated to most of the respiration involved enzymes (**Figure 4**). Previous studies conducted by our group on whole pears stored for long periods (6−8 months) under controlled atmosphere storage showed the same behavior (*7*, *9*). A complete down-regulation of these allergenic proteins was observed in browning inducing conditions of pear. Both in the current study on pear slices and in previous studies on whole pears allergens were down-regulated as the oxygen concentration dropped (*7*). In brown pear tissue (suboptimally stored under limiting levels of oxygen or high levels of carbon dioxide) the action of the enzyme PPO probably contributed to the total down-regulation of these allergenic proteins compared to the sound tissue (tissue that did not yet develop browning in pears showing the browning disorder). Thus, we suspect that total down-regulation of these allergenic proteins during CA storage of pears is to a certain extent correlated to the appearance of core breakdown. The possible role of these allergenic proteins during CA storage deserves further attention. Elucidation of their sequence, behavior, and abundance change of the different isoforms under different storage conditions should be performed in future studies using suitable MS approaches such as multiple reaction monitoring (MRM).

Polygalacturonase inhibiting protein (spot 165) was up-regulated under anoxic conditions. These results are in agreement with what we previously found with the long-term exposure of whole pears to different gas concentrations (*7*). It is possible that PGIP would have a dual role as PR proteins, conferring protection

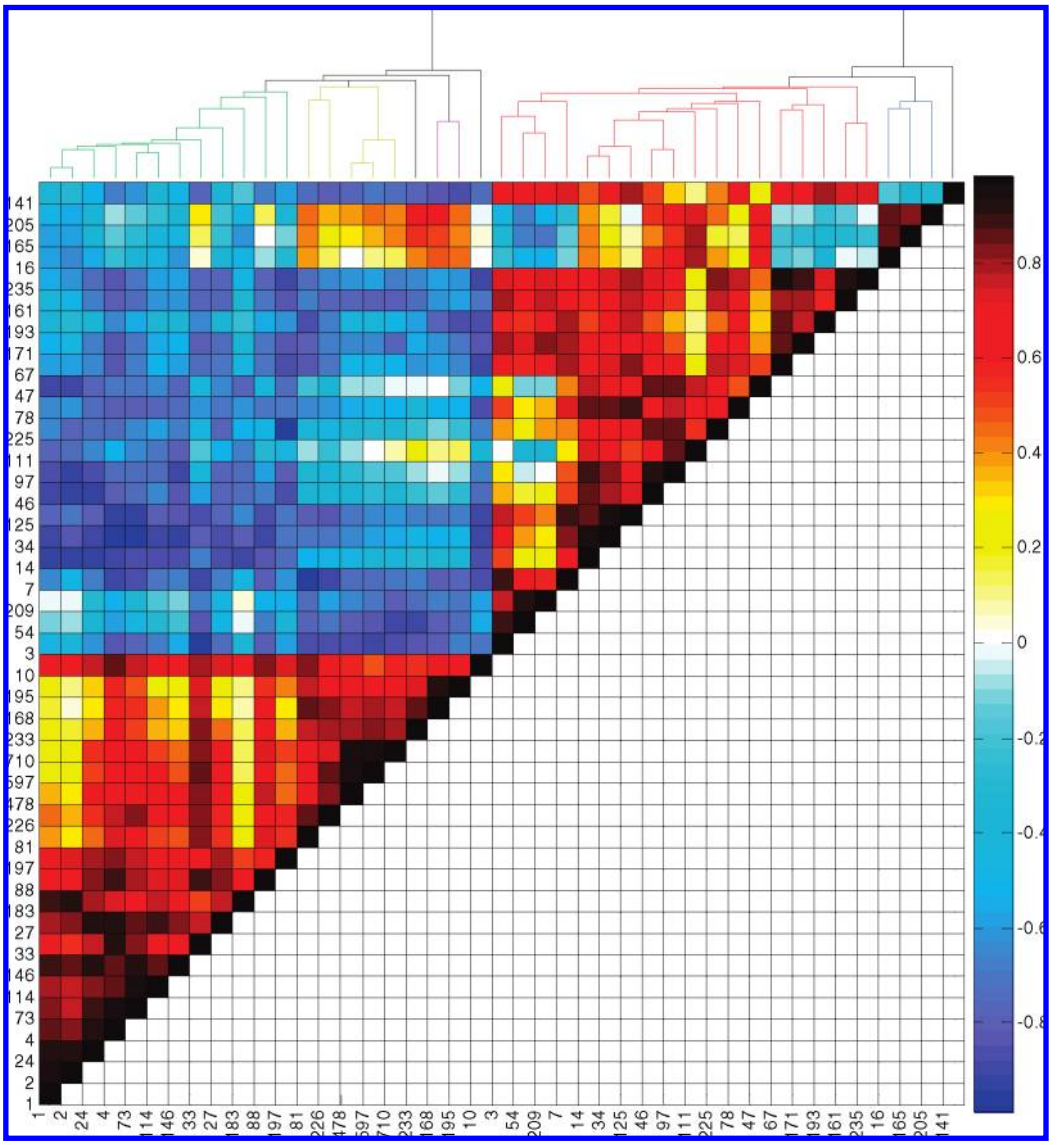

Figure 4. Correlation map for the 43 proteins identified as singlets by means of LC−ESI-MS/MS. Numbers represent the spot number of the proteins of **Table 1**. The color scale on the left goes from black "1", indicative of positive correlation, to blue "−1", indicative of negative correlation.

against pathogen attack and also during abiotic stress exposure (e.g., cold, anoxia).

Protein Synthesis. Protein synthesis is an ATP dependent process. Thus, it can be expected that under anoxic conditions, protein synthesis is down-regulated except for some specific anaerobic proteins. In this study, only two proteins involved in the synthesis of proteins (eukaryotic translation initiation factor eIF-4A, spots 146 and 73) were up-regulated under air conditions. Only, eIF-5A-2 (spot 16) was evidently up-regulated under anoxia (**Table 1**). Recently, it has been shown that eIF-5A-2 regulates programmed cell death caused by infection (*32*).

Conclusion. The current 2-DE DIGE approach studying extreme CA conditions on pear slices confirmed previous studies on whole pears in terms of regulation of proteins involved in respiration, protein synthesis, and defense mechanisms. In addition, anoxic conditions on pear slices revealed up-regulation of a pentose phosphate pathway enzyme as an alternative route for production of reducing equivalents for further defense mechanisms while skipping ATP consuming steps. The role of PR or allergenic proteins, as well as the polygalacturonase inhibiting protein, deserves further attention. They responded clearly to the extreme gas concentrations applied and were previously found to be relevant in the appearance of the physiological core breakdown disorder after long-term exposure of pears to suboptimal storage conditions.

ABBREVIATIONS

ANOVA, analysis of variance; CA, controlled atmosphere; CHAPS, 3-(3-cholamidopropyl)dimethylammonio-1propane sulfonate; DIGE, differential in gel electrophoresis; MRM, multiple reaction monitoring; DTT, dithiothreitol; IEF, isoelectric focusing; IPG, immobilized pH gradient; LV, latent variable; PC, principal component; PCA, principal component analysis; PGIP, polygalacturonase inhibiting protein; PLS-DA; partial least-squares discriminant analysis; PMT, photomultiplier tube; VIP, variable importance plot.

ACKNOWLEDGMENT

We thank Dr. Etienne Waelkens from (PROMETA, K. U. Leuven) for his support with the database searches.

Supporting Information Available: A Microsoft Excel spreadsheet contains results of the LC-ESI-MS/MS analysis,

and a Microsoft PowerPoint file contains the results of the PCA and PLS-DA models. This material is available free of charge via the Internet at http://pubs.acs.org.

LITERATURE CITED

(1) Gómez-Galindo, F.; Sjoholm, I. Plant stress physiology: opportunities and challenges for the food industry. *Crit. Rev. Food Sci. Nutr.* **2007**, *46*, 749–763.

(2) Gómez-Galindo, F.; Herppick, W.; Gekas, V.; Sjöholm, I. Factors affecting quality and postharvest properties of vegetables: integration of water relations and metabolism. *Crit. Rev. Food Sci. Nutr.* **2004**, *44*, 139–154.

(3) Kader, A. *Postharvest Biology and Technology of Horticultural Crops*; Division of Agriculture and Natural Resources, University of California: Oakland, CA, 2002; Vol. *3311*, pp 39−47.

(4) Kuo, S. J.; Parkin, L. Chilling injury in cucumbers associated with lipid peroxidation as measured by ethane evolution. *J. Food Sci.* **1989**, *54*, 1488–1491.

(5) Mohammed, M.; Wickham, L. D. Ocurrence of chilling injury in golden apples (*Spondias dulcis* Sonn.). *J. Food Qual.* **1997**, *20*, 91–104.

(6) Franck, C.; Lammertyn, J.; Ho, Q. T.; Verboven, P.; Verlinden, B.; Nicolaï, B. Review: Browning disorders in pear fruit. *Postharvest Biol. Technol.* **2007**, *43*, 1–13.

(7) Pedreschi, R.; Vanstreels, E.; Carpentier, S.; Hertog, M.; Lammertyn, J.; Robben, J.; Noben, J.; Swennen, R.; Vanderleyden, J.; Nicolaï, B. Proteomic analysis of core breakdown disorder in Conference pears (*Pyrus communis* L.). *Proteomics* **2007**, *7*, 2083–2099.

(8) Pedreschi, R.; Hertog, M.; Carpentier, S.; Lammertyn, J.; Robben, J.; Noben, J.; Panis, B.; Swennen, R.; Nicolaï, B. Treatment of missing values for multivariate statistical analysis of gel based proteomics data. *Proteomics* **2008**, *8*, 1371–1383.

(9) Pedreschi, R.; Hertog, M.; Robben, J.; Nobben, J. P.; Nicolaï, B. Proteomics to unravel the physiological implications of controlled atmosphere storage on Conference pears (*Pyrus communis L.*). *Postharvest Biol. Technol.* **2008**, *50*, 110–116.

(10) Pedreschi, R.; Franck, C.; Lammertyn, J.; Erban, A.; Kopka, J.; Hertog, M.; Nicolaï, B. Metabolic profiling of "Conference" pears under low oxygen stress. *Postharvest Biol. Technol.* **2009**, *51*, 123–130.

(11) Knee, M. Pome Fruit. In *Biochemistry of Fruit Ripening*; Seymour, G., Taylor, J., Tucker, G., Eds.; Chapman and Hall: London, U.K., 1993.

(12) Lammertyn, J.; Aerts, M.; Verlinden, B. E.; Schotsmans, W.; Nicolaï, B. Logistic regression analysis of factors influencing core breakdown in "Conference" pears. *Postharvest Biol. Technol.* **2000**, *20*, 25–37.

(13) Lammertyn, J.; Scheerlinck, N.; Jancsók, P.; Verlinden, B.; Nicolaï, B. A respiration−diffusion model for "Conference" pears I: model development and validation. *Postharvest Biol. Technol.* **2003**, *30*, 29–42.

(14) Lammertyn, J.; Scheerlinck, N.; Jancsók, P.; Verlinden, B.; Nicolaï, B. A respiration−diffusion model for "Conference" pears II: Simulation and relation to core breakdown. *Postharvest Biol. Technol.* **2003**, *30*, 43–55.

(15) Ho, Q. T.; Verlinden, B. E.; Verboven, P.; Vandewalle, S.; Nicolaï, B. A permeation−diffusion−reaction model of gas transport in cellular tissue of plant materials. *J. Exp. Bot.* **2006**, *57*, 4215–4224.

(16) Ho, Q. T.; Verlinden, B.; Verboven, P.; Vandewalle, S.; Nicolaï, B. A continuum model for gas exchange in pear fruit. *PloS Comput. Biol.* **2008**, *4*, e1000023.

(17) Verboven, P.; Kerckhofs, G.; Mebatsion, H. K.; Ho, Q. T.; Temst, K.; Wevers, M.; Cloetens, P.; Nicolaï, B. 3-D gas exchange pathways in pome fruit characterised by synchrotron X-ray computed tomography. *Plant Physiol.* **2008**, *147*, 518–527.

(18) Campostrini, N.; Areces, L.; Rappsilber, J.; Pietrogrande, C.; Dondi, F.; Pastorino, F.; Ponzoni, M.; Righetti, P. Spot overlapping in two-dimensional maps: a serious problem ignored for much too long. *Proteomics* **2005**, *5*, 2385–2395.

(19) Hunsucker, S. W.; Duncan, M. W. Is protein overlap in two-dimensional gels a serious practical problem? *Proteomics.* **2006**, *6*, 1374–1375.

(20) Liu, H.; Sadygov, R. G.; Yates, J. R. A model for random sampling and estimation of relative protein abundance in shotgun proteomics. *Anal. Chem.* **2004**, *76*, 4193–4201.

(21) Deutsch, E. W.; Lam, H.; Aebersold, R. Data analysis and bioinformatics tools for tandem mass spectrometry in proteomics. *Physiol. Genomics* **2008**, *33*, 18–25.

(22) Karp, N.; McCormick, P. S.; Russell, M. R.; Lilley, K. S. Experimental and statistical considerations to avoid false conclusions in proteomics studies using differential in-gel electrophoresis. *Mol. Cell. Proteomics* **2007**, *6*, 1354–1364.

(23) Storey, J. D.; Tibshirani, R. Statistical significance for genomewide studies. *Proc. Natl. Acad. Sci. U.S.A.* **2003**, *100*, 9440–9445.

(24) Johnson, A. R.; Wichern, W. D. *Applied Multivariate Statistical Analysis*; Prentice Hall: Upper Saddle River, NJ, 1998.

(25) Coulthurst, S. J.; Lilley, K. S.; Hedley, P. E.; Liu, H.; Toth, I. K.; Salmond, G. DsbA plays a critical and multifaceted role in the production of secreted virulence factors by the phytopathogen *Erwinia carotenova* subsp. *Atroseptica*. *J. Biol. Chem.* **2008**, *283*, 23739–23753.

(26) Lu, P.; Vogel, C.; Wang, R.; Yao, X.; Marcotte, E. Absolute protein expression profiling estimates the relative contributions of transcriptional and translational regulation. *Nat. Biotechnol.* **2007**, *25*, 117–124.

(27) Xia, Q.; Hendrickson, E. L.; Wang, T.; Lamont, R. J.; Leigh, J. A.; Hackett, M. Review: Protein abundance ratios for global studies of prokaryotes. *Proteomics* **2007**, *7*, 2904–2919.

(28) Nesvizhskii, A.; Vitek, O.; Aebersold, R. Analysis and validation of proteomic data generated by tandem mass spectrometry. *Nat. Methods* **2007**, *4*, 787–797.

(29) Colinge, J.; Chiappe, D.; Lagache, S.; Moniatte, M. Differential proteomics via probabilistic peptide identification scores. *Anal. Chem.* **2005**, *77*, 596–606.

(30) Yang, Y.; Thannhauser, T. W.; Li, L.; Zhang, S. Development of an integrated approach for evaluation of 2-D gel image analysis: impact of multiple proteins in single spots on comparative proteomics in conventional 2-D gel/MALDI workflow. *Electrophoresis* **2007**, *28*, 2080–2094.

(31) Kruger, N. J.; von Schaewen, A. The oxidative pentose phosphate pathway: structure and organization. *Curr. Opin. Plant Biol.* **2003**, *6*, 236–246.

(32) Thompson, J. E. eIF5A is involved in pathogen-induced cell death and development of disease symptoms in *Arabidopsis thaliana*. *Plant Physiol.* **2008**, *148*, 479–489.

Received February 5, 2009. Revised manuscript received June 22, 2009. Accepted June 22, 2009. This research has been carried out in the framework of EU COST action 924. R.P. extends acknowledgment to the International Relations Office of K. U. Leuven (IRO scholarship).